# SANDIA REPORT

NUREG/CR–3635
SAND84–8715
R1
Printed June 1984

# Simulation of Flame Propagation Through Vorticity Regions Using the Discrete Vortex Method

(Presented at the Symposium on Fluid Dynamics, April 26-27, 1984, at the Department of Mechanical and Industrial Engineering, University of Illinois at Urbana-Champaign)

P. K. Barr

Prepared by
Sandia National Laboratories
Albuquerque, New Mexico 87185 and Livermore, California 94550
for the United States Department of Energy
under Contract DE-AC04-76DP00789

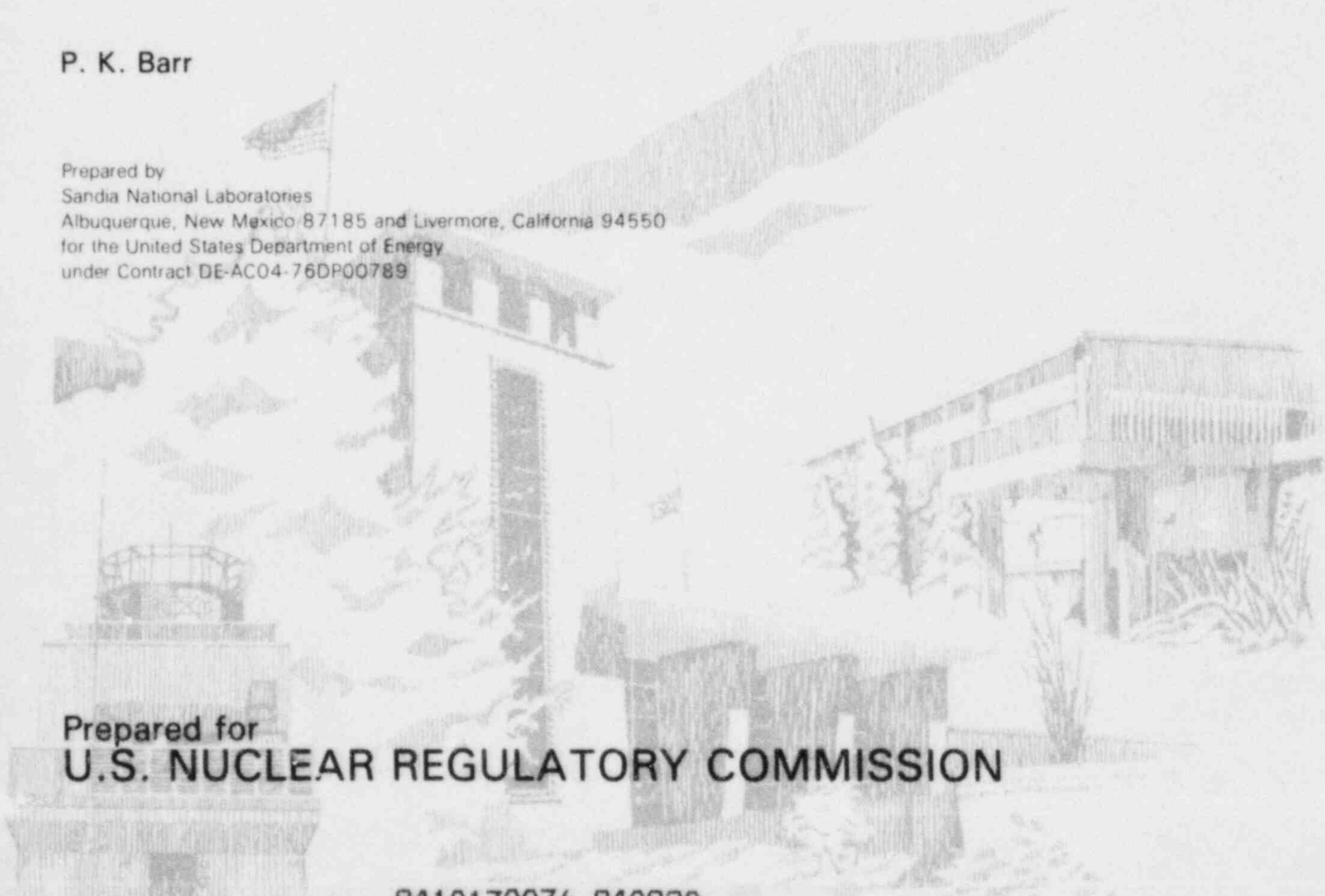

**Prepared for**
**U.S. NUCLEAR REGULATORY COMMISSION**



SF 2900-Q(6-82)

NUREG/CR-3835
SAND84-8715
R1

# SIMULATION OF FLAME PROPAGATION THROUGH VORTICITY REGIONS USING THE DISCRETE VORTEX METHOD

P. K. Barr

June 1984

Sandia National Laboratories
Livermore, CA 94550
Operated by
Sandia Corporation
for the
U. S. Department of Energy

Prepared for
Division of Accident Evaluation
U. S. Nuclear Regulatory Commission
Washington, DC 20555
Under Memorandum of Understanding DOE 40-550-75
NRC FIN No. A1246

**SIMULATION OF FLAME PROPAGATION THROUGH VORTICITY REGIONS USING THE DISCRETE VORTEX METHOD***

P. K. Barr
Sandia National Laboratories
Livermore, California 94550

ABSTRACT

The interaction of a freely propagating premixed flame with regions of high vorticity in the flow is investigated using a computer model. These vorticity regions are formed due to the flame-generated volume expansion that pushes gas past obstacles ahead of the flame. In the computer model the discrete vortex dynamics method is used to simulate the time development of the vorticity regions downstream of each obstacle. The flame front is modeled as a wrinkled laminar flame interface that propagates normal to itself at the laminar burning velocity, separating the two different density fluids: burned and unburned. Two different obstacle configurations are discussed in this paper. In the first case, a flame causes unburned gas to exhaust out of a planar duct, and when the flame reaches the duct exit it interacts with the vorticity which was formed at the exit. Two versions of this configuration are considered: sharp and square edge exit. The second case involves a series of obstacles in a channel. Here, the repeated obstacles in the channel leads to acceleration of the flame as indicated by the dramatic increase in fuel consumption.

* Partially supported by the U. S. Nuclear Regulatory Commission and the U. S. Department of Energy, Office of Basic Energy Sciences.

CONTENTS

## INTRODUCTION

For premixed flame propagation the fuel consumption rate depends on both the surface area of the flame and the local flame speed. The flame surface area can be greatly increased by convection in a turbulent flow region. In partially confined flows, the chemically-induced volume expansion determines the strength of the turbulence regions downstream of obstacles in the flame's path. Thus, as the flame surface area increases, the strength of the turbulence also increases, creating a positive feedback which further accelerates the flame. Accidents that create a combustible gas within a confined or semiconfined volume create a dangerous situation if obstacles such as large equipment, ventilation ducts, or doorways between rooms are present. The presence of these obstacles can lead to an acceleration of the rate of combustion, possibly resulting in pressures which exceed the design limit of the confining structure.

Moen, et al. (1980) demonstrated that the presence of repeated obstacles in the path of a freely propagating flame has significant effect on the rate of flame propagation. This positive feedback mechanism can lead to explosive hazards. Experiments by Lee, et. al. (1983) have shown that the presence of the obstacles in small tubes can provide a mechanism by which the flame can transit to detonation, even though the initial ignition source was not strong enough to initiate a detonation. It is this process of flame interaction with the repeated obstacles that generates enough energy release to detonate the remaining gas mixture.

The work presented here deals with the numerical modeling of this flame acceleration mechanism.

## COMPUTER SIMULATION

This computer model deals with the phenomena associated with flame propagation in a planar channel containing baffles. The presence of obstacles causes two events that act to increase the burning rate. One is the contraction of the streamlines as the flow goes over each obstacle. This causes the flame surface to elongate as the flow carries the flame through the obstacle-created contraction, increasing the surface area and thus the burning rate. The second effect is the formation of a standing eddy downstream of the obstacles.

In this work the discrete vortex dynamics method is combined with a flame propagation algorithm to model this phenomena. The formation of the eddy regions behind the obstacles is simulated by introducing discrete vorticity into the flow field at the ends of the obstacles. The strength of each discrete vortex is governed by both the frequency of vortex shedding (time interval for integration) and the magnitude of the velocity past the obstacle (velocity change through the boundary layer). In this model, no other mechanism is included which can change the amount of vorticity present in the flow (i.e., boundary layers along other walls, vorticity creation along the flame front, etc.).

A premixed combustible gas is assumed, and chemical kinetics is replaced with a simple flame model that propagates a flame interface into the unburned gas at a specified speed, in this case the laminar burning velocity (see Barr and Ashurst, 1983). A fixed numerical mesh is used to record the location of burned and unburned mixture, and the flame interface is reconstructed from this information. The size of the mesh imposes a lower limit on the resolution of flame wrinkling.

The assumption of constant pressure in the flow field results in the restriction to low speed flows, that is, below Mach 0.4. The velocity potential resulting from the volume expansion is governed by the Poisson equation. However, the geometry of the obstacle configuration produces an irregular domain for the flow field. In order to solve the Poisson equation over this domain, a fast Poisson solver capable of handling these irregular boundaries is used (Grcar, 1983).

## FLAME PROPAGATION THROUGH A SINGLE VORTICITY REGION

The first case considered is the effect of a single vorticity region on the propagation of the flame (see Figure 1). In this case, only minor confinement is imposed by two solid perpendicular walls and a shorter third wall which forms a channel. Point ignition occurs at the closed end of this channel, and the gas that expands during combustion pushes flow down the channel, past the edge of the channel, and out through the free boundaries. This flow past the edge of the channel exit causes a continuous sheet of vorticity to be released into the flow, and because of the quiescent initial conditions and dimensions of the channel, forms a single vortex (see Yip, et al., 1984). This vortex grows in size and strength as the gas continues to flow out the channel exit.

In the computer simulation this continuous sheet of vorticity is modeled by shedding many discrete vortices, resulting in an overlap of their regions of influence and thus a smooth distribution of vorticity. As can be seen in Figure 1, the individual vortices, indicated by dashed lines scaled to their velocities (which in this case overlap), act to form a single vorticity region. The flame represents a discontinuity in density, the ratio of the unburned to the burned density being 7:1. As the flame propagates down this channel, it moves at a fairly constant velocity until it starts to interact with the vorticity. The swirling motion distorts the flame, increasing its surface area and thus the burning rate. The flame spirals towards the center of the vorticity, leaving separate spirals of burned and unburned fluid, until the flame has consumed the unburned fluid within the vorticity region.

Similar behavior is observed in the case of a square-edged channel, as indicated in Figure 2. In this case, all parameters are the same as those for Figure 1, except the channel exit geometry. Here, the individual vortices are released at the same location as that for the run in Figure 1. However, in this case the eddy formation is affected by the vertical edge of the channel, as is the spiraling of the flame front as it interacts with the vorticity region. Since in the model a slip boundary condition is used along the additional vertical wall, it merely acts to block the flow. A comparison of these results with experimental results is underway (Strehlow, 1984).

## FLAME PROPAGATION THROUGH MULTIPLE CHAMBER GEOMETRIES

The acceleration of the flame as it interacts with flow over a series of obstacles is demonstrated in Figure 3a, which presents a series of computer-generated movie frames separated by equal time intervals. In this case the flame propagates around four staggered obstacles in a channel open only along the right edge. The combustible mixture is ignited along the left wall at the closed end of the channel and expands at a density ratio of 3.8:1. The frames in Figure 3a show the development of the turbulent recirculation regions and indicate the speed with which the flame moves through the channel. Figure 3b presents additional frames from this movie, showing details of the flame propagation over the obstacles. As can be seen in these figures, the acceleration of the flame does not start until it begins to pass around the first obstacle. The increase in the flame surface area due to channel area contraction at each obstacle and interaction with the shed vortices causes the flame to accelerate, as can be seen from the relative positions of the flame front in each succeeding picture.

Experimental results of flame propagation in multiple chambers has been reported by Chan, et al. (1983). In this experiment, the chamber is a 60 cm long channel (12.7 cm square cross section) containing planar baffles and is open at one end. It is filled with a mixture of 10.6% hydrogen in air and is ignited along the closed end. The side walls are transparent, allowing for Schlieren cinematography to be used to record the flame motion. The comparison of these experimental results with the computational results is encouraging (see Chan, et al., 1983). In both, the flame front jets through the center of the channel, and enhanced burning takes place behind each of the obstacles. Comparisons of computed flow velocities with point measurements of gas speeds has indicated that the rate of acceleration in the numerical simulation is too low, perhaps by a factor of two. The quantity used in the comparison should be the net flux through the outlet, or some other quantity that reflects the overall burning rate. However, a comparison of the experimental and numerical flame shapes at similar front positions has indicated that smaller scale turbulence may be present in the experimental results, resulting in increased burning in the shear regions behind the obstacles.

## CONCLUSION

The effect of obstacles in the presence of a freely propagating premixed flame under varying degrees of partial confinement has been numerically simulated. The time development of the eddy regions downstream of each obstacle is accomplished with the aid of discrete vortex dynamics. The flame, modeled as an interface between the burned and unburned fluid, is treated as a wrinkled laminar flame. This simulation, though limited to low speed flows, includes the significant effects which result in the initial acceleration of a flame as it propagates over obstacles.

Computational results of flame propagation over a single obstacle and over a series of obstacles, both of which were discussed in this paper, demonstrate the capabilities of the method. Future extensions of this work will include quantitative comparison with experimental results (see Chan, et al., 1983, and Strehlow, 1984). Results from these comparisons will result in improvements in the flame propagation simulation, either to include flame extinction due to the local flow parameters, or to simulate the effects of the fine scale turbulence present in the repeated obstacle experiments.

## ACKNOWLEDGEMENT

The author would like to thank Dr. W. T. Ashurst for his continued assistance with the vortex dynamics method.

## REFERENCES

Barr, P.K. and Ashurst, W.T., (1983), "An Interface Scheme for Turbulent Flame Propagation," Sandia National Laboratories Report SAND82-8773.

Chan, C.K., Lee, J.H.S., Barr, P. and Ashurst, W., (1983), "Flame Acceleration in Multiple Chambers," presented at the 1983 Technical Meeting of the Eastern Section of the Combustion Institute (November 8-10), Paper 50.

Dugger, G.L., and Graab, D.D., (1953) "Flame Velocities of Hydrocarbon-Oxygen-Nitrogen Mixtures," Fourth Symposium (International) on Combustion, Combustion Institute, pp. 302-310.

Grcar, J.F., Sandia National Laboratories, Livermore, California, private communication (1983).

Lee, J.H.S., Knystautas, R., Chan, C., Barr, P.K., Grcar, J.F., and Ashurst, W.T., (1983), "Turbulent Flame Acceleration: Mechanisms and

Computer Modeling," presented at the International Meeting on Light-Water Reactor Severe Accident Evaluation, Cambridge, MA, August 28 - September 1, 1983, Paper 9.8, sponsored by ANS and ENS; also Sandia National Laboratories Report SAND83-8655.

Moen, I.O., Donato, M., Knystautas, R., and Lee, J.H., (1980), "Flame Acceleration Due to Turbulence Produced by Obstacles," Combustion and Flame, **39**, pp 21-32.

Strehlow, R.A., University of Illinois at Urbana-Champaign, private communication, March 1984.

Yip, T.W.G., Strehlow, R.A., and Ormsbee, A.I., (1984) "An Experimental Investigation of Two Dimensional Flame-Vortex Interactions," accepted at Twentieth Symposium (International) on Combustion, the Combustion Institute.

## FIGURE CAPTIONS

**Figure 1.** Frames from a computer-generated movie of flame propagation through a single vorticity region formed at the exit of a channel. Time sequence proceeds vertically from the lower left, and to the right by columns. First frame shown is 2.5 msec after point ignition occurred at the closed end of the channel. Gas is assumed to be stoichiometric propane-air mixture plus 10% oxygen which has a laminar burning velocity of 94 cm/sec (Duggar and Graab, 1953). Ratio of unburned to burned gas density is 7:1, grid size is 200-by-100. Thirty computational time steps separate the frames shown; shedding of discrete vorticity occurs during every time step.

**Figure 2.** Frames from a computer-generated movie of flame propagation through a single vorticity region formed at the exit of a square-edged channel. All parameters similar to those in Figure 1.

**Figure 3a.** Flame acceleration through a four-chamber configuration. The distortion in the flame shape as it approaches the first of a series of obstacles increases the flow velocity which, combined with the vorticity, further increases the flame surface. The discrete vorticity is shown by dashed lines, which are scaled to the velocity vector. The combustible mixture is 10.6% hydrogen in air which has a laminar burning velocity of 40 cm/sec (though it is very sensitive to hydrogen concentration), and the ratio of unburned to burned gas density is 3.8:1. Ignition occurred along left wall (top frame), time between plots is 30 msec. Channel is 12.7 cm in height and 60 cm long. Grid size is 179-by-40.

**Figure 3b.** Additional frames from the movie described in Figure 3a. Top plot is at a time of 110 msec. The smaller time interval, 3 msec between plots, reveals flame shape during its passage between chambers.

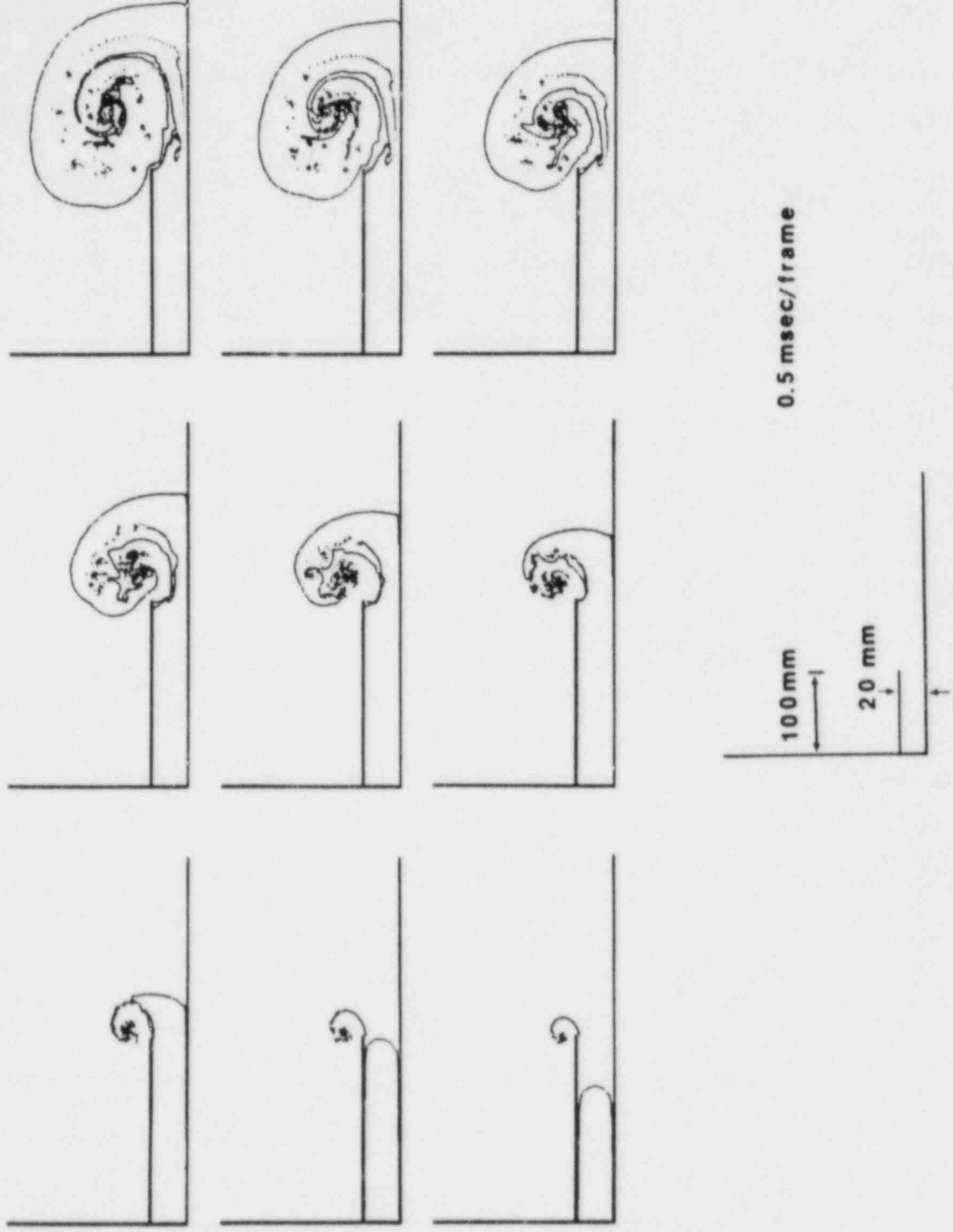


Figure 1

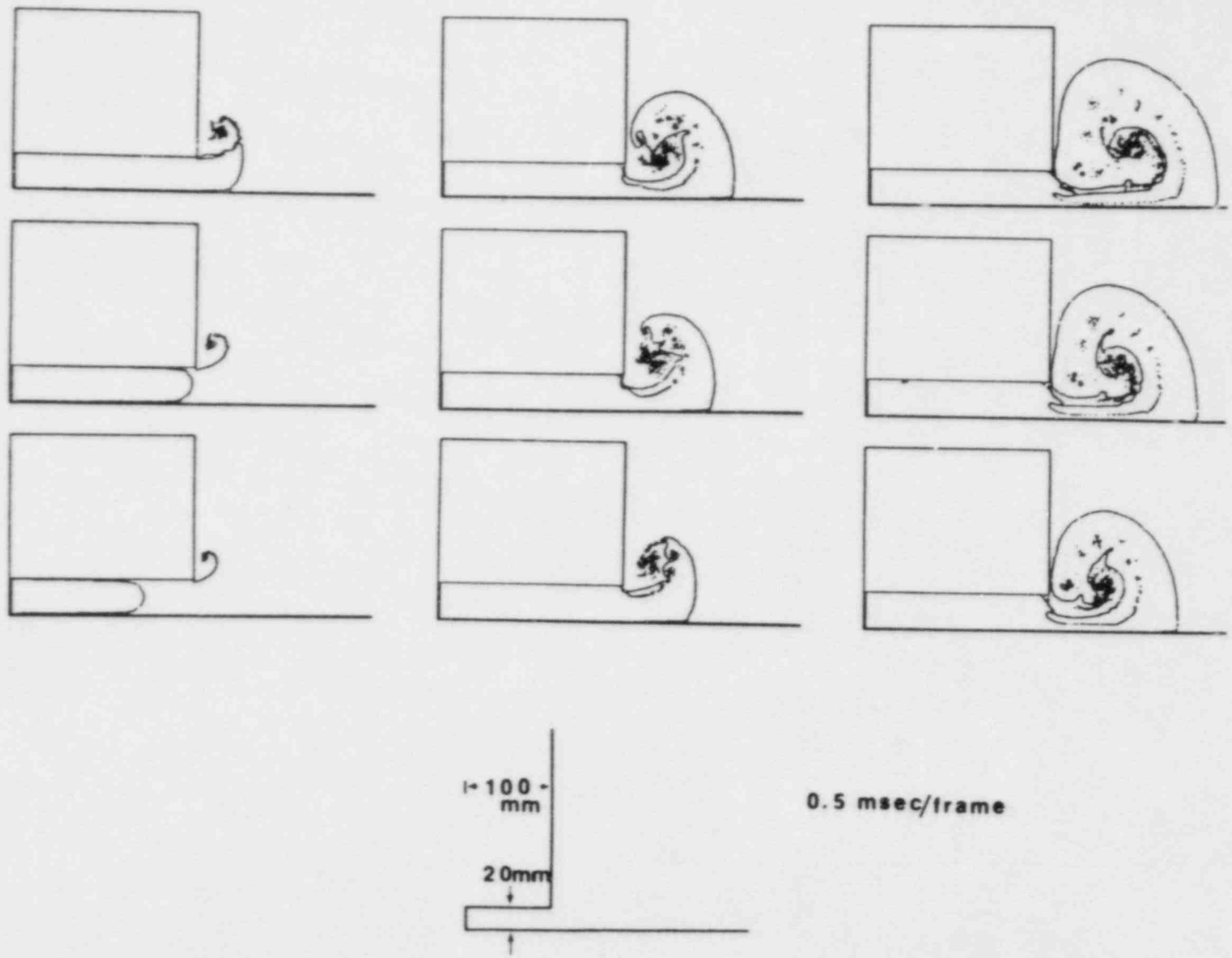


Figure 2

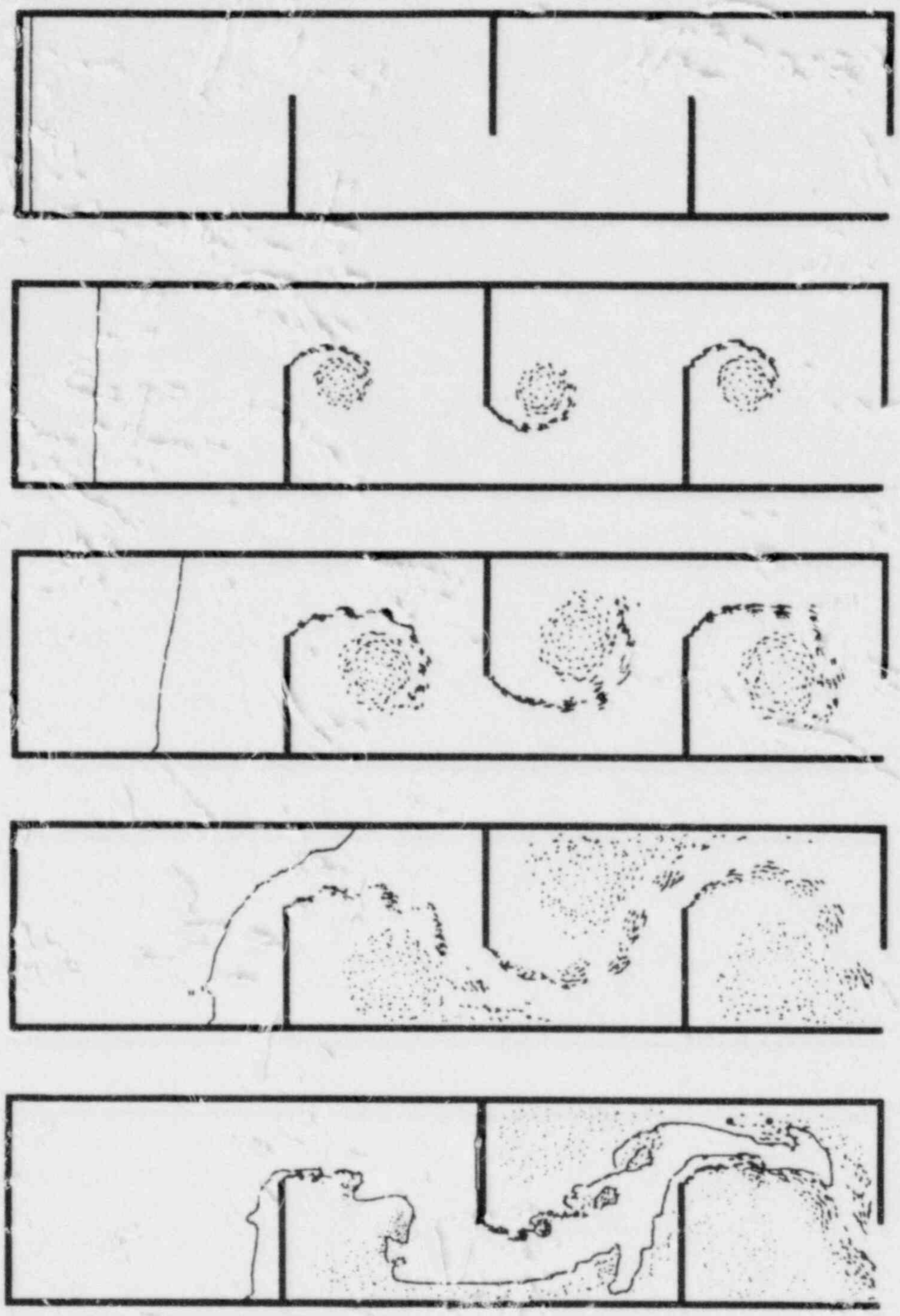

Figure 3a

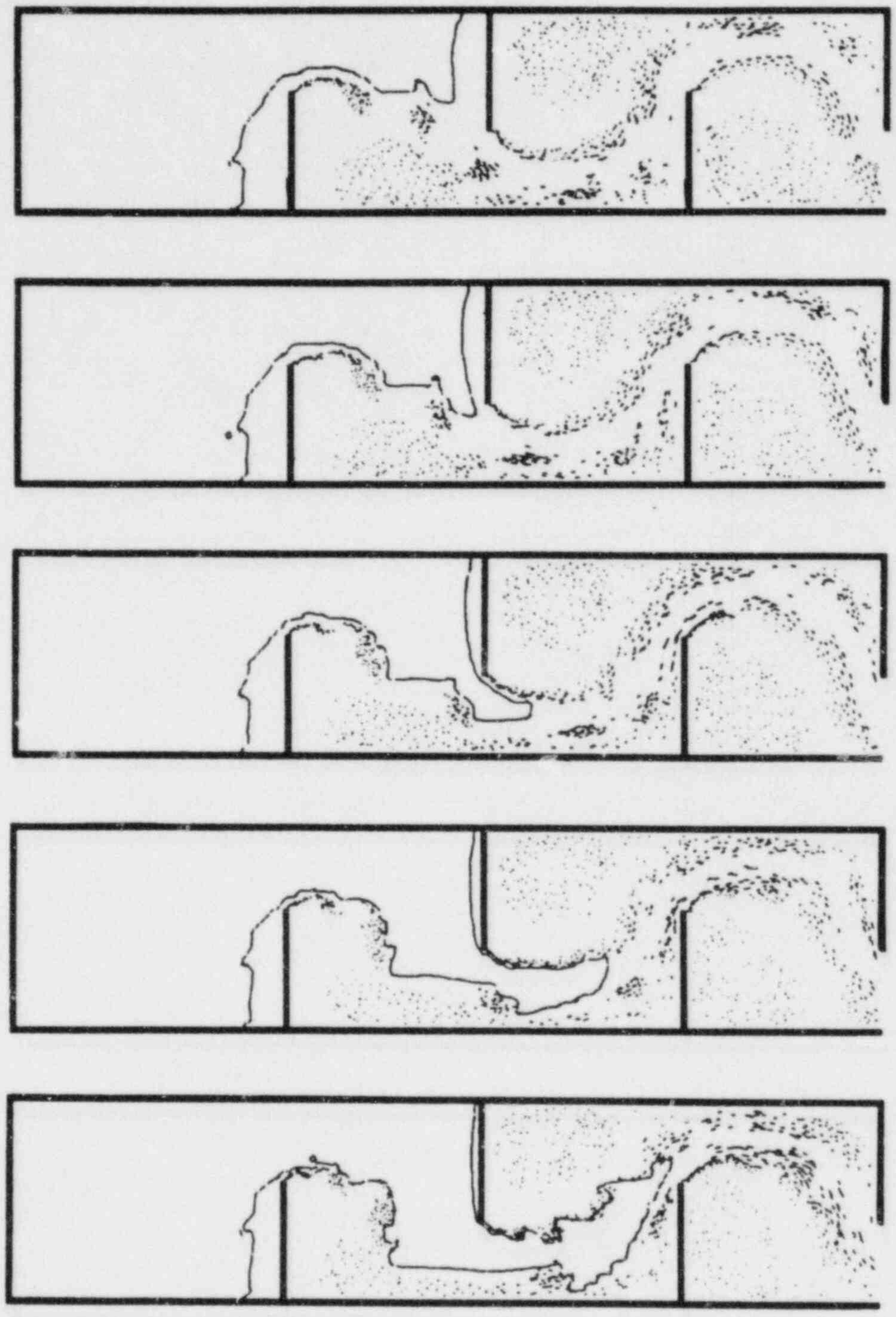

Figure 3b

DISTRIBUTION:

U. S. NRC Distribution Contractor
15700 Crabbs Branch Way
Rockville, MD 20850
(275 copies for R1)

W. G. Agnew
Technical Director
General Motors Research Center
Twelve Mile & Mound Roads
Warren, MI 48090

C. Anderson
Dept. of Mathematics
Stanford University
Stanford, CA 94305

R. E. Balzhiser
Vice President, EPRI
P. O. Box 10412
Palo Alto, CA 94308

W. Bartok
Scientific Advisor
Exxon Research and Engineering
P. O. Box 45
Linden, NJ 07036

J. T. Beale
Mathematics Dept.
Duke University
Durham, NC 27706

R. W. Bilger
Mechanical Engineering
University of Sydney
N.S.W. 2006, Australia

K. N. C. Bray
Aeronautics & Astronautics
University of Southampton
Southampton, SO9 6NH England

C. Chan
Mechanical Engineering
McGill University
817 Sherbrooke St. W.
Montreal, Quebec
Canada H3A 2K6

R. Chevray
Mechanical Engineering
State University of New York
Stony Brook, NY 11794

A. Chorin
Mathematics Department
University of California
Berkeley, CA 94720

P. Clavin
Laboratoire de Dynamique
et Thermophysique des Fluides
Universite de Provence
Centre de St-Jerome
13397 Marseille Cedex 13 France

L. Cloutman
T-3, MS-B216
Los Alamos National Laboratory
Los Alamos, NM 87545

P. Colella, 50A - 2113
Lawrence Berkeley Laboratory
Berkeley, CA 94720

W. D. Compton
Vice President Research Staff
Ford Motor Company
P. O. Box 2053, Rm S2106
Dearborn, MI 48121

H. A. Dwyer
Mechanical Engineering
University of California
Davis, CA 95616

R. Fristrom
Johns Hopkins Applied Physics Lab.
Johns Hopkins Road
Laurel, MD 20810

W. C. Gardiner
Department of Chemistry
University of Texas
Austin, TX 78712

A. F. Ghoniem
Mech. Engr. Dept., Rm 3-339
Mass. Institute of Technology
Cambridge, MA 02139

N. B. Hannay
2219 Fir Lane
Mitchell Point
Friday Harbor, WA 98250

J. M. Hyman
T-7, MS-B284
Los Alamos National Laboratory
Los Alamos, NM 87545

R. J. Kandel
Chemical Sciences Division
Office of Energy Research
Department of Energy
Washington, D.C. 20545

J. A. Kezerle
Combustion Chemistry
Gas Research Institute
8600 West Bryn Mawr Avenue
Chicago, IL 60631

W. Kollmann
Mechanical Engineering
University of California
Davis, CA 95616

J. T. Larkins
US Nuclear Regulatory Commission
Severe Accident Assessment Branch
7915 Easton Ave.
Silver Spring, MD 20910

A. H. Laufer
Room G334 - DOE
1000 Independence Ave. S. W.
Washington, DC 20545

J. H. S. Lee
Mechanical Engineering
McGill University
817 Sherbrooke St. W.
Montreal, Quebec
Canada H3A 2K6

A. Leonard
NASA-Ames Research Center
Moffet Field, CA 94035

P. Libby
Applied Mechanics
& Engineering Sciences
University of California
P. O. Box 109
La Jolla, CA 92037

M. Linevsky
Johns Hopkins Applied Physics Lab.
Johns Hopkins Road
Laurel, MD 20810

J. P. Longwell
Chem. Engr. Dept., Rm 66554
Mass. Institute of Technology
Cambridge, MA 02139

O. Manley
Division of Engineering,
Mathematical & Geosciences
Office of Basic Energy Sciences
Department of Energy
Washington, D.C. 20545

B. Matkowsky
Engineering Science &
Applied Mathematics
The Technological Institute
Northwestern University
Evanston, IL 60201

A. K. Oppenheim
Mechanical Engineering
University of California
Berkeley, CA 94720

A. Ormsbee
Dept. of Aeronautics
University of Illinois
Urbana, IL 61801

H. B. Palmer
College of Earth & Mineral Sciences
Fuel Science Section
The Pennsylvania State University
101 Mineral Industries Building
University Park, PA 16802

S. S. Penner
Energy Center B-010
University of California San Diego
La Jolla, CA 92093

N. Peters
Institut for
Allgemeine Mechanik
RWTH Aachen
Templergraben 64
5100 Aachen,
Fed. Rep. of Germany

J. Ramshaw
T-Division
Los Alamos National Laboratory
Los Alamos, NM 87544

J. Ross
Department of Chemistry
Stanford University
Stanford, CA 94305

R. F. Sawyer
Mechanical Engineering
Universiy of California
Berkeley, CA 94720

J. Sethian
50A-2129
Lawrence Berkeley Lab.
Berkeley, CA 94720

W. A. Sirignano
Mechanical Engineering
Carnegie-Mellon University
Schenley Park
Pittsburgh, PA 15213

W. P. Slichter
Executive Director
Research-Materials Science
and Engineering Division
Bell Laboratories
600 Mountain Avenue
Murray Hill, NJ 07974

R. A. Strehlow
Dept. of Aeronautics
University of Illinois
Urbana, IL 61801

F. Dee Stevenson
Chemical Sciences Division
Office of Energy Research
Department of Energy
Washington, D.C. 20545

C. Tinkler
US Nuclear Regulatory Commission
Containment Systems Branch
7920 Norfolk Avenue
Bethesda, MD 20014

F. A. Williams
Aerospace & Mechanical Sciences
Princeton University
D-207 Engineering Quadangle
Princeton, NJ 08546

P. Worthington
US Nuclear Regulatory Commission
Chemical Engineering Branch
Division of Engineering Technology
5650 Nicholson Lane
Rockville, MD 20852

S. T. Zalesak
Naval Research Laboratory
Washington, D.C. 20375

W. F. Noh, LLNL, L71

C. K. Westbrook, LLNL, L71

P. R. Woodward, LLNL, L71

T. B. Cook, 20

J. W. Nunziato, 1510

J. C. Cummings, 1512

M. R. Baer, 1513

D. B. Hayes, 2530

A. W. Snyder, 6400

J. V. Walker, 6420

M. Berman, 6427

S. L. Thompson, 6444

R. S. Claassen, 8000

D. M. Olson, 8100

C. M. Hartwig, 8124

M. E. John, 8125

A. N. Blackwell, 8200

R. J. Kee, 8231

J. F. Grcar, 8231

S. B. Margolis, 8231

L. R. Petzold, 8231

D. L. Hartley, 8300

P. L. Mattern, 8350

S. C. Johnston, 8351

W. J. McLean, 8353

R. J. Cattolica, 8353

S. Vosen, 8353

C. W. Robinson, 8360

D. R. Hardesty, 8361

T. M. Dyer, 8362

B. R. Sanders, 8363

W. T. Ashurst, 8363

P. K. Barr, 8363 (15)

A. A. Borja, 8363

A. R. Kerstein, 8363

N. N. Mansour, 8363

K. D. Marx, 8363

L. Gutierrez, 8400

Publications Div., 8265/Technical
  Library Processes Division, 3141

Technical Library Processes
  Division, 3141 (3)

M. A. Pound, 8424-2 for Central
  Technical Files (3)

| Org. | Bldg. | Name | Rec'd by | Org. | Bldg. | Name | Rec'd by |
|---|---|---|---|---|---|---|---|
| | | | | | | | |

120555078877 1 1AN1R1
US NRC
ADM-DIV OF TIDC
POLICY & PUB MGT BR-PDR NUREG
W-501
WASHINGTON DC 20555

Sandia National Laboratories